

Quadratic canonical transformation theory and higher order density matrices

Eric Neuscamman¹, Takeshi Yanai, and Garnet Kin-Lic Chan

Citation: *J. Chem. Phys.* **130**, 124102 (2009); doi: 10.1063/1.3086932

View online: <http://dx.doi.org/10.1063/1.3086932>

View Table of Contents: <http://aip.scitation.org/toc/jcp/130/12>

Published by the [American Institute of Physics](#)

Quadratic canonical transformation theory and higher order density matrices

Eric Neuscamman,^{1,a)} Takeshi Yanai,² and Garnet Kin-Lic Chan¹¹*Department of Chemistry and Chemical Biology, Cornell University, Ithaca, New York 14850, USA*²*Institute of Molecular Science, 38 Nishigo-Naka, Myodaiji, Okazaki 444-8585, Japan*

(Received 15 December 2008; accepted 3 February 2009; published online 23 March 2009)

Canonical transformation (CT) theory provides a rigorously size-extensive description of dynamic correlation in multireference systems, with an accuracy superior to and cost scaling lower than complete active space second order perturbation theory. Here we expand our previous theory by investigating (i) a commutator approximation that is applied at quadratic, as opposed to linear, order in the effective Hamiltonian, and (ii) incorporation of the three-body reduced density matrix in the operator and density matrix decompositions. The quadratic commutator approximation improves CT's accuracy when used with a single-determinant reference, repairing the previous formal disadvantage of the single-reference linear CT theory relative to singles and doubles coupled cluster theory. Calculations on the BH and HF binding curves confirm this improvement. In multireference systems, the three-body reduced density matrix increases the overall accuracy of the CT theory. Tests on the H₂O and N₂ binding curves yield results highly competitive with expensive state-of-the-art multireference methods, such as the multireference Davidson-corrected configuration interaction (MRCI+Q), averaged coupled pair functional, and averaged quadratic coupled cluster theories. © 2009 American Institute of Physics. [DOI: 10.1063/1.3086932]

I. INTRODUCTION

Molecules where the electrons are strongly correlated represent a challenging class of systems for quantitative quantum chemistry due to the non-mean-field character of their wave functions. Such systems are termed multireference, due to the necessity of incorporating multiple electronic configurations in order to achieve a correct qualitative description. Examples of multireference problems are abundant, and include the chemistry of bond breaking, excited states, and transition metal compounds. While methods such as complete active space self-consistent field^{1,2} and, recently, the density matrix renormalization group³⁻⁷ (DMRG) provide good descriptions of the *nondynamic*, or qualitative, correlations of multireference systems, they need to be augmented with a description of the instantaneous, or *dynamic*, electron correlations to provide quantitative predictions. In single-reference problems, where all electron correlation is dynamic in nature, coupled cluster (CC) methods are known to provide affordable accuracy and reliability.⁸⁻¹⁰ In multireference problems, however, there currently exist no dynamic correlation methods that provide the same balance of accuracy and reliability that coupled cluster methods have brought to single-reference systems.

Historically, dynamic correlation methods for multireference systems have fallen into two broad categories. The first is second order perturbation theory, including complete active space second order perturbation theory (CASPT2),¹¹⁻¹³ multireference Moller-Plesset theory,¹⁴ and more recently *n*-electron valence perturbation theory.^{15,16} The most widely used of these is CASPT2, but this unfortunately has both

lower accuracy and a higher cost scaling in multireference systems (with reasonable active spaces) than singles and doubles CC theory does for single-reference systems. This higher cost scaling becomes a particular problem when large active spaces are employed, as is common in DMRG calculations. Furthermore, CASPT2 can sometimes have issues of reliability due to the problem of intruder states.¹⁷ The second category of methods for treating multireference dynamic correlation includes the multireference configuration interaction¹⁸⁻²⁰ (MRCI) and closely related coupled pair functional theories. MRCI is the simple extension of configuration interaction to use a multideterminant reference, and it inherits the lack of size extensivity common to configuration interaction methods. Various corrections have been developed that address the size-extensivity issue, such as the Davidson correction (MRCI+Q),^{21,22} the averaged coupled pair functional,^{23,24} and averaged quadratic coupled cluster theory.²⁵ While these corrected methods are significantly more accurate than MRCI, they are still not rigorously size extensive except in certain limits. MRCI based methods have even higher cost scalings than perturbation theory, which limits their application to small systems. When they can be applied, however, the corrected MRCI methods are generally reliable and very accurate.

Canonical transformation (CT) theory²⁶⁻²⁸ is designed to model dynamic correlation in large multireference systems while meeting three important criteria: rigorous size-extensivity, a cost scaling equivalent to CCSD, and accuracy for multireference systems comparable to what CCSD provides for single-reference systems. CT theory uses a unitary exponential ansatz, which is also used in unitary CC theory,²⁹⁻³⁵ some multireference CC theories,^{36,37} van Vleck-

^{a)}Electronic mail: eric.neuscamman@gmail.com.

type perturbation theories as explored by Freed³⁸ and Kirtman,³⁹ and White's⁴⁰ earlier canonical diagonalization theory. The central object in CT theory is the effective Hamiltonian (as in canonical diagonalization theory) which is Hermitian as a result of using the unitary exponential. Low cost scaling is achieved by making approximations to the commutators that appear in the nonterminating Baker–Campbell–Hausdorff (BCH) expansion of the effective Hamiltonian and in the amplitude equations. The commutator approximation uses a decomposition of many body operators and reduced density matrices (RDMs) into combinations of one- and two-body operators and RDMs. Different CT theories can be derived by employing different operators and RDM decompositions, although the current form of CT theory uses the theory of extended normal ordering of Mukherjee and co-workers^{41–43} and the theory of cumulants.^{44–46} A central feature of the commutator approximation is that the resulting CT amplitude and energy equations can be evaluated with only the one- and two-body RDMs of the reference system, a significant advantage in systems with large active spaces. Taken together, the unitary exponential, effective Hamiltonian, and commutator approximation result in a CT theory that is rigorously size extensive and has a cost scaling equivalent to CCSD, *but for multireference problems*.

Our previous papers^{26,27} have defined the linear CT method with singles and doubles (LCTSD), where linear indicates the order in the BCH expansion at which the first commutator approximation is employed. In addition to size extensivity and favorable cost scaling, LCTSD has displayed excellent accuracy in multireference systems. For bond breaking in H₂O, N₂, and FeO, LCTSD's accuracy is decisively superior to CASPT2 and often competitive with the corrected MRCI theories, while being of substantially lower cost. This paper proposes two extensions of the existing LCTSD method. The first is the *quadratic commutator approximation*, which can replace the linear commutator approximation where applicable, to give the quadratic canonical transformation theory with singles and doubles, or QCTSD method. This higher order commutator approximation removes the formal weaknesses of single-reference LCTSD as compared to CCSD theory. The second is the incorporation of *exact three-body RDMs* for systems in which they are available, which gives (when combined with the linear or quadratic commutator approximations) the L3CTSD and Q3CTSD methods. The incorporation of three-body RDM information is naturally expected to improve the accuracy of the CT method in especially difficult multireference problems, but still requires less cost than existing multireference configuration interaction theories. Finally, we also investigate in detail numerical issues of convergence that arise when solving the CT amplitude equations, and propose some practical solutions.

It is important at this point to distinguish the use of cumulants in CT theory from their use in other methods. Cumulant approximations are most commonly used in quantum chemistry by contracted Schrödinger equation (CSE) methods,^{47–49} which directly optimize a system's one- and two-body RDMs. In these methods, cumulants are employed

to approximate the three- and/or four-body RDMs. This approximation can lead to many problems, one of which is the dependence of *n*-representability error on basis set size as explored by Harris⁵⁰ and Herbert.⁵¹ CT theory also approximates the three- and four-body RDMs using cumulants, but only in the active space and only for the reference wave function (as opposed to CSE methods which approximate the final wave function's RDMs in both the active and external spaces). This should remove problems of basis set dependence, as the reference wave function's active space RDMs change little with the basis set. Indeed, previous results²⁷ show that CT theory's accuracy is not affected when changing from a double- to triple-zeta basis set in the nitrogen dimer. An additional difference from CSE methods is that CT theory optimizes an excitation operator (as in CC theory) rather than the system's RDMs. It is therefore reasonable to expect *n*-representability problems to be less prevalent. Another method whose use of cumulants bears similarity to CT theory is Mazziotti's anti-Hermitian contracted Schrödinger equation method,^{52–54} although there the focus is on the two-body RDM rather than an effective Hamiltonian.

We begin our theoretical discussion with a general review of CT theory (Sec. II A) and an explanation of the central idea of decomposing many body operators and RDMs (Sec. II B). We then describe in detail the LCTSD (Sec. II C), QCTSD (Sec. II D), and L3CTSD and Q3CTSD (Sec. II E) theories. Next comes a perturbative analysis of how QCTSD improves the formal properties of CT theory in single-reference problems (Sec. II F). We conclude our theoretical discussion with a description of the numerical stability issue and how it is addressed (Sec. II G). In the methods section (Sec. III) we describe the automatic derivation and implementation of the complicated functions required by quadratic CT theory. Finally (Sec. IV) we present results and analysis for four benchmark molecular curves: BH, HF, H₂O, and N₂.

II. THEORY

A. Overview

As in unitary CC theory, CT theory seeks to find the unitary transformation that maps a reference wave function onto the true wave function, as shown in Eq. (1). This reference function may consist of one or more electronic configurations, allowing CT theory to treat both single- and multi-reference problems.

$$|\Psi\rangle = e^A|\Psi_0\rangle. \quad (1)$$

In singles and doubles CT, the unitary transformation is built from the exponential of antisymmetric single and double excitation operators. This set of operators, which excludes those containing more than two core or two virtual indices, as well as those with only active indices, is shown in Eq. (2). We refer to the operator coefficients as amplitudes.

$$A = \sum_{i_1 s_1} A_{i_1}^{s_1} (a_{i_1}^{s_1} - a_{s_1}^{i_1}) + \sum_{\substack{i_2 i_3 \\ s_2 s_3}} A_{i_2 i_3}^{s_2 s_3} (a_{i_2 i_3}^{s_2 s_3} - a_{s_2 s_3}^{i_2 i_3}),$$

$$a_{i_1}^{s_1} = a_{s_1}^\dagger a_{i_1}, \quad (2)$$

$$a_{i_2 i_3}^{s_2 s_3} = a_{s_2}^\dagger a_{s_3}^\dagger a_{i_3} a_{i_2}.$$

In this paper we distinguish between core orbitals (index label c) which are doubly occupied in all of the reference function's configurations, active orbitals (a) which may have any occupation, and virtual orbitals (v) which are unoccupied in the reference. We also define the indices i as ranging over core and active, s over active and virtual, and e over core and virtual orbitals, while p and q are treated as general indices.

CT theory applies the unitary operator to the Hamiltonian to create an effective Hamiltonian and the corresponding effective Schrödinger equation, Eqs. (3) and (4).

$$\bar{H} = e^{-A} H e^A = H + [H, A] + \frac{1}{2!} [[H, A], A] + \dots, \quad (3)$$

$$\bar{H}|\Psi_0\rangle = E|\Psi_0\rangle. \quad (4)$$

The amplitudes are determined by solving the nonlinear amplitude equations, Eqs. (5) and (6), which take the form of generalized Brillouin conditions.⁵⁵

$$\langle \Psi_0 | [\bar{H}, a_{i_1}^{s_1} - a_{s_1}^{i_1}] | \Psi_0 \rangle = 0, \quad (5)$$

$$\langle \Psi_0 | [\bar{H}, a_{i_2 i_3}^{s_2 s_3} - a_{s_2 s_3}^{i_2 i_3}] | \Psi_0 \rangle = 0. \quad (6)$$

The central idea in CT theory is to introduce a two-body approximation of \bar{H} by applying a commutator approximation to the BCH expansion and amplitude equations. This allows the amplitudes and energy to be determined using only the one- and two-body RDMs. The precise definition of three-body to two-body decompositions used in the commutator approximation leads to different variants of CT theory.

B. Operator and density matrix decomposition

In CT theory we decompose many body operators and RDMs into combinations of lower body operators and RDMs. The rules for doing so are based on the theory of cumulants⁴⁵ and the extended-normal-ordered (ENO) operators of Kutzelnigg and Mukherjee.⁴¹ A three-body operator, for example, can be expressed as a constant plus a collection of one-, two-, and three-body ENO operators. The ENO operators have a zero expectation value with respect to an arbitrary (possibly multireference) reference function, just as traditionally normal-ordered particle creation and destruction operators have a zero expectation value with respect to the true vacuum. In CTSD, we neglect all ENO operators of order greater than two. In an analogous manner, the three-body RDM can be written as a collection of one-, two-, and three-body cumulants, and by neglecting the three-body cumulant we may approximate it using one- and two-body RDMs.

To begin, let us consider Eqs. (7) and (8), which decompose the three-body RDM and operator into their one- and two-body approximations. These equations are derived by neglecting the three-body cumulant and ENO operator from their defining equations in Ref. 41. The notation $X_{1,2}$ implies the decomposition of X into one- and two-body RDMs and operators.

$$(\gamma_{q_1 q_2 q_3}^{p_1 p_2 p_3})_{1,2} = \sum (-1)^x \gamma_{q_1}^{p_1} \gamma_{q_2 q_3}^{p_2 p_3} \quad (9 \text{ terms})$$

$$- 2 \sum (-1)^x \gamma_{q_1}^{p_1} \gamma_{q_2}^{p_2} \gamma_{q_3}^{p_3} \quad (6 \text{ terms}), \quad (7)$$

$$(a_{q_1 q_2 q_3}^{p_1 p_2 p_3})_{1,2} = \sum (-1)^x \gamma_{q_1}^{p_1} a_{q_2 q_3}^{p_2 p_3} \quad (9 \text{ terms})$$

$$+ \sum (-1)^x \gamma_{q_1 q_2}^{p_1 p_2} a_{q_3}^{p_3} \quad (9 \text{ terms})$$

$$- 2 \sum (-1)^x \gamma_{q_1}^{p_1} \gamma_{q_2}^{p_2} a_{q_3}^{p_3} \quad (18 \text{ terms})$$

$$- \sum (-1)^x \gamma_{q_1}^{p_1} \gamma_{q_2 q_3}^{p_2 p_3} \quad (9 \text{ terms})$$

$$+ 4 \sum (-1)^x \gamma_{q_1}^{p_1} \gamma_{q_2}^{p_2} \gamma_{q_3}^{p_3} \quad (6 \text{ terms}). \quad (8)$$

These equations make use of the notation $\sum (-1)^x A_{q_1 q_2 \dots}^{p_1 p_2 \dots} B_{q_k q_{k+1} \dots}^{p_k p_{k+1} \dots}$, which implies that there is one term for each unique partitioning of the indices among the objects (A, B, \dots) in which p_i are kept on top and q_i on bottom. For each permutation of the indices from their original positions, a factor of (-1) is applied. Equations (9) and (10) give examples of this rule.

$$\sum (-1)^x \gamma_{q_1}^{p_1} a_{q_2 q_3}^{p_2 p_3} = \gamma_{q_1}^{p_1} a_{q_2 q_3}^{p_2 p_3} - \gamma_{q_1}^{p_2} a_{q_2 q_3}^{p_1 p_3} - \gamma_{q_1}^{p_3} a_{q_2 q_3}^{p_1 p_2}$$

$$- \gamma_{q_2}^{p_1} a_{q_1 q_3}^{p_2 p_3} + \gamma_{q_2}^{p_2} a_{q_1 q_3}^{p_1 p_3} - \gamma_{q_2}^{p_3} a_{q_1 q_3}^{p_1 p_2}$$

$$- \gamma_{q_3}^{p_1} a_{q_2 q_1}^{p_2 p_3} - \gamma_{q_3}^{p_2} a_{q_1 q_2}^{p_1 p_3} + \gamma_{q_3}^{p_3} a_{q_1 q_2}^{p_1 p_2}, \quad (9)$$

$$\sum (-1)^x \gamma_{q_1}^{p_1} \gamma_{q_2}^{p_2} \gamma_{q_3}^{p_3} = \gamma_{q_1}^{p_1} \gamma_{q_2}^{p_2} \gamma_{q_3}^{p_3} - \gamma_{q_1}^{p_1} \gamma_{q_2}^{p_2} \gamma_{q_3}^{p_3} - \gamma_{q_1}^{p_1} \gamma_{q_2}^{p_2} \gamma_{q_3}^{p_3}$$

$$- \gamma_{q_2}^{p_1} \gamma_{q_1}^{p_2} \gamma_{q_3}^{p_3} + \gamma_{q_2}^{p_1} \gamma_{q_3}^{p_2} \gamma_{q_1}^{p_3} + \gamma_{q_3}^{p_1} \gamma_{q_1}^{p_2} \gamma_{q_2}^{p_3}. \quad (10)$$

Decompositions of the three-body RDM and operators (7) and (8) were used in Ref. 27 to define the Mukherjee-Kutzelnigg variant of the LCTSD theory. In this work, we explore a quadratic commutator approximation which also requires decompositions for four-body RDMs and operators. Using the same notation, these are shown in Eqs. (11) and (12).

$$(\gamma_{q_1 q_2 q_3 q_4}^{p_1 p_2 p_3 p_4})_{1,2} = \sum (-1)^x \gamma_{q_1 q_2}^{p_1 p_2} \gamma_{q_3 q_4}^{p_3 p_4} \quad (18 \text{ terms})$$

$$- 2 \sum (-1)^x \gamma_{q_1}^{p_1} \gamma_{q_2}^{p_2} \gamma_{q_3}^{p_3} \gamma_{q_4}^{p_4} \quad (24 \text{ terms}), \quad (11)$$

$$\begin{aligned}
(a_{q_1 q_2 q_3 q_4}^{p_1 p_2 p_3 p_4})_{1,2} &= \sum (-1)^x \gamma_{q_1 q_2}^{p_1 p_2} a_{q_3 q_4}^{p_3 p_4} \quad (36 \text{ terms}) \\
&- 2 \sum (-1)^x \gamma_{q_1}^{p_1} \gamma_{q_2}^{p_2} \gamma_{q_3}^{p_3} a_{q_4}^{p_4} \quad (96 \text{ terms}) \\
&- \sum (-1)^x \gamma_{q_1 q_2}^{p_1 p_2} \gamma_{q_3 q_4}^{p_3 p_4} \quad (18 \text{ terms}) \\
&+ 6 \sum (-1)^x \gamma_{q_1}^{p_1} \gamma_{q_2}^{p_2} \gamma_{q_3}^{p_3} \gamma_{q_4}^{p_4} \quad (24 \text{ terms}).
\end{aligned} \tag{12}$$

We will also investigate systems for which the exact three-body RDM can be practically computed. In such cases, the more accurate decompositions given in Eqs. (13)–(15) may be used. These are derived by neglecting all three- and four-body ENO operators and all four-body cumulants. The notation $X_{1,2,(3)}$ implies the decomposition of X into one-, two-, and three-body RDMs and one- and two-body operators.

$$\begin{aligned}
(a_{q_1 q_2 q_3}^{p_1 p_2 p_3})_{1,2,(3)} &= \sum (-1)^x \gamma_{q_1}^{p_1} a_{q_2 q_3}^{p_2 p_3} \quad (9 \text{ terms}) \\
&+ \sum (-1)^x \gamma_{q_1 q_2}^{p_1 p_2} a_{q_3}^{p_3} \quad (9 \text{ terms}) \\
&- 2 \sum (-1)^x \gamma_{q_1}^{p_1} \gamma_{q_2}^{p_2} a_{q_3}^{p_3} \quad (18 \text{ terms}) \\
&- 2 \sum (-1)^x \gamma_{q_1}^{p_1} \gamma_{q_2 q_3}^{p_2 p_3} \quad (9 \text{ terms}) \\
&+ 6 \sum (-1)^x \gamma_{q_1}^{p_1} \gamma_{q_2}^{p_2} \gamma_{q_3}^{p_3} \quad (6 \text{ terms}) \\
&+ \gamma_{q_1 q_2 q_3}^{p_1 p_2 p_3},
\end{aligned} \tag{13}$$

$$\begin{aligned}
(\gamma_{q_1 q_2 q_3 q_4}^{p_1 p_2 p_3 p_4})_{1,2,(3)} &= \sum (-1)^x \gamma_{q_1}^{p_1} \gamma_{q_2 q_3 q_4}^{p_2 p_3 p_4} \quad (16 \text{ terms}) \\
&+ \sum (-1)^x \gamma_{q_1 q_2}^{p_1 p_2} \gamma_{q_3 q_4}^{p_3 p_4} \quad (18 \text{ terms}) \\
&- 2 \sum (-1)^x \gamma_{q_1}^{p_1} \gamma_{q_2}^{p_2} \gamma_{q_3 q_4}^{p_3 p_4} \quad (72 \text{ terms}) \\
&+ 6 \sum (-1)^x \gamma_{q_1}^{p_1} \gamma_{q_2}^{p_2} \gamma_{q_3}^{p_3} \gamma_{q_4}^{p_4} \quad (24 \text{ terms}),
\end{aligned} \tag{14}$$

$$\begin{aligned}
(a_{q_1 q_2 q_3 q_4}^{p_1 p_2 p_3 p_4})_{1,2,(3)} &= \sum (-1)^x \gamma_{q_1 q_2}^{p_1 p_2} a_{q_3 q_4}^{p_3 p_4} \quad (36 \text{ terms}) \\
&+ \sum (-1)^x \gamma_{q_1 q_2 q_3}^{p_1 p_2 p_3} a_{q_4}^{p_4} \quad (16 \text{ terms}) \\
&- \sum (-1)^x \gamma_{q_1}^{p_1} \gamma_{q_2 q_3}^{p_2 p_3} a_{q_4}^{p_4} \quad (144 \text{ terms}) \\
&- \sum (-1)^x \gamma_{q_1 q_2}^{p_1 p_2} \gamma_{q_3 q_4}^{p_3 p_4} \quad (18 \text{ terms}) \\
&+ 6 \sum (-1)^x \gamma_{q_1}^{p_1} \gamma_{q_2}^{p_2} \gamma_{q_3}^{p_3} \gamma_{q_4}^{p_4} \quad (24 \text{ terms}).
\end{aligned} \tag{15}$$

A final note is that the decompositions in Eqs. (7)–(15) are invariant to unitary rotations within the active orbitals, which should render CT theory invariant as well. In practice, however, the numerical truncation discussed in Sec. II G removes this invariance, as noted previously.²⁶

C. Linear CTSD

The LCTSD method derives from the application of the linear commutator approximation $[X, Y]_{1,2}$ to the BCH expansion (3) and amplitude equations (5) and (6). Equation (16) displays the approximate BCH expansion, in which three-body operators are decomposed after each commutator.

$$\bar{H} = H + [H, A]_{1,2} + \frac{1}{2!} [[H, A]_{1,2}, A]_{1,2} + \dots \tag{16}$$

This expansion can be evaluated recursively by using the result of each term as the input for the next term. While the recursion is formally infinite, at some order the terms become negligible because A , which treats only dynamic correlation, is typically small.

The value of the amplitude Brillouin condition for an excitation operator \hat{o} [where \hat{o} is e.g., $a_{i_2 i_3}^{s_2 s_3} - a_{s_2 s_3}^{i_2 i_3}$, see Eqs. (5) and (6)] which we call the residual with respect to \hat{o} , is approximated in LCTSD by Eq. (17).

$$R(\hat{o}) = \langle [\bar{H}, \hat{o}]_{1,2} \rangle. \tag{17}$$

For simplicity we have omitted the reference Ψ_0 from the expression for the expectation value. Note that while $\langle [\bar{H}, \hat{o}]_{1,2} \rangle$ is equivalent to $\langle [\bar{H}, \hat{o}]_{1,2} \rangle$, it is implemented separately in our code for reasons of efficiency.

To obtain the amplitudes, LCTSD solves the amplitude equations through a Newton–Raphson scheme with step-size control and an approximate Jacobian. Computing the true Jacobian matrix would require differentiating each amplitude equation with respect to each amplitude, but the approximation to the Jacobian’s action shown in Eq. (18) is sufficient.

$$(J\vec{x})_{\hat{o}} = \langle [[\bar{H}, X]_{1,2}, \hat{o}]_{1,2} \rangle. \tag{18}$$

Here \vec{x} is the vectorized set of amplitudes corresponding to the amplitude operator X , while $(J\vec{x})_{\hat{o}}$ refers to the amplitude corresponding to the excitation operator \hat{o} in the vector produced by acting J on \vec{x} . Using this approximation to the Jacobian’s action, the amplitudes are computed iteratively using Eq. (19).

$$J(\vec{x}_{i+1} - \vec{x}_i) = -\vec{r}_i. \tag{19}$$

Here \vec{x}_i and \vec{r}_i are the vectorized amplitudes and residuals for the i th iteration, while \vec{x}_{i+1} are the vectorized amplitudes for the $(i+1)$ th iteration (before applying step-size control).

D. Quadratic CTSD

The QCTSD method arises from using both the linear $[X, Y]_{1,2}$ and quadratic $[[X, Y], Z]_{1,2}$ commutator approximations to obtain the effective Hamiltonian and amplitude equations. The distinction from LCTSD arises from the fact that quadratic terms $[[X, Y]_{1,2}, Z]_{1,2}$ in LCTSD involve two successive decompositions, and are not equivalent to the corre-

sponding terms $[[X, Y], Z]_{1,2}$ involving only a single decomposition, as used in QCTSD. The resulting form of \bar{H} arising in QCTSD is displayed in Eq. (20).

$$\begin{aligned} \bar{H} = & H + [H, A]_{1,2} + \frac{1}{2!} [[H, A], A]_{1,2} \\ & + \frac{1}{3!} [[[[H, A], A]_{1,2}, A]_{1,2}]_{1,2} + \frac{1}{4!} [[[[[[H, A], A]_{1,2}, A]_{1,2}, A]_{1,2}]_{1,2}]_{1,2} \\ & + \dots \end{aligned} \quad (20)$$

A subtle consequence of the decompositions in QCTSD is that by separating the Hamiltonian into its one- and two-body constituents (h_1 and h_2), we can exploit the fact that $[h_1, A]$ is expressed exactly with one- and two-body operators, to delay the operator decomposition of commutators involving h_1 to one higher order in A . This gives rise to a modified form of the QCTSD effective Hamiltonian \bar{H} which we shall use in this work, shown in Eqs. (21)–(23).

$$\bar{H} = H + \bar{H}^{(1)} + \bar{H}^{(2)}, \quad (21)$$

$$\begin{aligned} \bar{H}^{(1)} = & [h_1, A] + \frac{1}{2!} [[h_1, A], A]_{1,2} + \frac{1}{3!} [[[[h_1, A], A]_{1,2}]_{1,2}]_{1,2} \\ & + \frac{1}{4!} [[[[[[h_1, A], A]_{1,2}, A]_{1,2}, A]_{1,2}]_{1,2}]_{1,2} + \dots, \end{aligned} \quad (22)$$

$$\begin{aligned} \bar{H}^{(2)} = & [h_2, A]_{1,2} + \frac{1}{2!} [[h_2, A], A]_{1,2} \\ & + \frac{1}{3!} [[[[h_2, A], A]_{1,2}, A]_{1,2}]_{1,2} \\ & + \frac{1}{4!} [[[[[[h_2, A], A]_{1,2}, A]_{1,2}, A]_{1,2}, A]_{1,2}]_{1,2} + \dots \end{aligned} \quad (23)$$

The residual in QCTSD is also defined using both the linear and quadratic commutator approximations. As discussed above, we can distinguish between the h_1 and h_2 contributions, and thus we determine the QCTSD residuals via Eqs. (24)–(26).

$$R(\hat{\rho}) = R^{(1)}(\hat{\rho}) + R^{(2)}(\hat{\rho}), \quad (24)$$

$$\begin{aligned} R^{(1)}(\hat{\rho}) = & \langle [h_1, \hat{\rho}] \rangle + \langle [[h_1, A], \hat{\rho}]_{1,2} \rangle \\ & + \frac{1}{2!} \langle [[[[h_1, A], A]_{1,2}, \hat{\rho}]_{1,2}]_{1,2} \rangle + \dots, \end{aligned} \quad (25)$$

$$\begin{aligned} R^{(2)}(\hat{\rho}) = & \langle [h_2, \hat{\rho}]_{1,2} \rangle + \langle [[h_2, A], \hat{\rho}]_{1,2} \rangle \\ & + \frac{1}{2!} \langle [[[[h_2, A], A]_{1,2}, \hat{\rho}]_{1,2}]_{1,2} \rangle + \dots \end{aligned} \quad (26)$$

A final difference between QCTSD and LCTSD is the evaluation of the Jacobian's action, for which QCTSD simply removes the decomposition from the inner commutator of Eq. (18), giving Eq. (27).

$$(J\vec{x})_{\hat{\rho}} = \langle [[\bar{H}, X], \hat{\rho}]_{1,2} \rangle \quad (27)$$

TABLE I. Commutators and cost scalings for various methods. Costs assume that active space size is proportional to system size. For CASPT2 and MRCI, the first cost assumes an uncontracted theory requiring the CI coefficients, while the second assumes a fully contracted theory requiring only the RDMs. For very large active spaces, diagonalizing the semi-internal overlap matrix will increase the cost of CT and contracted CASPT2 to $O(n^9)$.

Method	Commutators	Cost
CCSD	...	$O(n^6)$
LCTSD	$[H, A]_{1,2}$	$O(n^6)$
QCTSD	$[H, A]_{1,2} [[H, A], A]_{1,2}$	$O(n^6)$
L3CTSD	$[H, A]_{1,2,(3)}$	$O(n^7)$
Q3CTSD	$[H, A]_{1,2,(3)} [[H, A], A]_{1,2,(3)}$	$O(n^8)$
CASPT2	...	$O(e^n)$ or $O(n^8)$
MRCI	...	$O(e^n)$ or $O(n^{10})$

We conclude our discussion of QCTSD by noting that although it is a more expensive method than LCTSD, it retains the same cost scaling. The difference in cost between evaluating the linear and quadratic commutator approximations $[H, A]_{1,2}$ and $[[H, A], A]_{1,2}$ is a constant factor only.

E. Incorporating three-body RDMs

Both the linear and quadratic algorithms can be made more accurate by incorporating the exact three-body RDM. This is accomplished by replacing the decompositions in Eqs. (7), (8), (11), and (12) with those in Eqs. (13)–(15). We formulate the L3CTSD algorithm by making the substitutions shown in Eqs. (28) and (29) to the BCH expansion and residual equation of LCTSD.

$$[H, A]_{1,2} \rightarrow [H, A]_{1,2,(3)}, \quad (28)$$

$$\langle [H, \hat{\rho}] \rangle_{1,2} \rightarrow \langle [H, \hat{\rho}] \rangle. \quad (29)$$

In the same manner, Q3CTSD is derived from QCTSD through the substitutions shown in Eqs. (28)–(31).

$$[[H, A], A]_{1,2} \rightarrow [[H, A], A]_{1,2,(3)}, \quad (30)$$

$$\langle [[H, A], \hat{\rho}] \rangle_{1,2} \rightarrow \langle [[H, A], \hat{\rho}] \rangle_{1,2,(3)}. \quad (31)$$

Here the subscript 1,2,(3) denotes the decomposition of three- and higher-body operators and four- and higher-body RDMs into one- and two-body operators and one-, two-, and three-body RDMs.

While LCTSD and QCTSD both have cost scalings equivalent to CCSD, the incorporation of the three-body RDM increases the scalings of L3CTSD and Q3CTSD, as shown in Table I. This makes the three-body RDM methods less feasible in large systems, especially those with large active spaces. We note, however, that the cost scalings of L3CTSD and Q3CTSD are still lower than that of MRCI-type methods.

F. Perturbative analysis of QCTSD for a single-determinant reference

This section continues the discussion presented in Ref. 26, where the CT energy was analyzed via perturbation

theory for the special case in which the reference function is a single determinant. The analysis is carried out with respect to the Fermi vacuum (particle-hole transformation), where the occupied orbital destruction and creation operators are transformed to hole creation and destruction operators, respectively, while virtual orbital creation and destruction operators are viewed as particle creation and destruction operators. With this substitution, any normal-ordered operator will have a zero expectation value with respect to the reference determinant. As a result, all RDMs are identically zero in the Fermi vacuum. This property has an important consequence for the operator decompositions of Eqs. (8) and (12). By setting the RDMs to zero, we see that decomposing a three- or four-body operator in the Fermi vacuum is equivalent to neglecting the operator altogether.

Writing the Hamiltonian as $H = E_{\text{HF}} + F + W$, we separate the one-body Fock operator F from the two-body fluctuation W . We also separate our amplitude operator into one- and two-body components via $A = A_1 + A_2$. By applying Brillouin's theorem to the amplitude equations, one can show that A_1 is second order in W while A_2 is first order. From these properties, the previous paper demonstrated that LCTSD's largest energy error is of order W^4 . Here we demonstrate that QCTSD's largest error is of order W^5 . In comparison, the largest error in CCSD involving the one- and two-body excitation operators T_1 and T_2 is also W^5 .⁵⁶ Note that the L3CTSD and Q3CTSD methods are redundant here, because the decomposition of the 3-body RDM is exact for a single-determinant reference.

Before proving our result for QCTSD, let us consider LCTSD's treatment of the BCH term $[[W, A_2], A_2]$ as an example of how we analyze CT's perturbative accuracy. LCTSD approximates this term as $[[W, A_2]_{1,2}, A_2]_{1,2}$. In the Fermi vacuum, this approximation is equivalent to neglecting the three-body operators after each commutator. Since the RDMs are zero, only full contractions resulting from the commutators will contribute to the energy. Thus the outer decomposition produces no error. Further, any three-body operator produced by the inner commutator cannot fully contract during the outer commutator, and so the inner decomposition is also error-free.

Now consider the order W^4 BCH terms, which are shown in Eq. (32).

$$\begin{aligned}
 E^{(4)} = & \left\langle \frac{1}{2} [[W, A_1], A_2] + \frac{1}{2} [[W, A_2], A_1] + \frac{1}{2} [[F, A_1], A_1] \right. \\
 & + \frac{1}{6} [[[F, A_1], A_2], A_2] + \frac{1}{6} [[[F, A_2], A_1], A_2] \\
 & + \frac{1}{6} [[[F, A_2], A_2], A_1] + \frac{1}{6} [[[W, A_2], A_2], A_2] \\
 & \left. + \frac{1}{24} [[[[F, A_2], A_2], A_2], A_2] \right\rangle. \quad (32)
 \end{aligned}$$

By the same reasoning as in our example above, LCTSD computes the correct energy contribution for all terms in Eq. (32) except the last two. The first error is caused by decomposing (neglecting) the three-body operator produced by the innermost commutator of the term $[[[W, A_2], A_2], A_2]$. This operator can fully contract during the outer two commutators and thus has a nonzero energy contribution. In contrast, QCTSD approximates this term as $[[[W, A_2], A_2]_{1,2}, A_2]_{1,2}$. No error results from neglecting the three- and four-body

operators produced by the second commutator, as they cannot fully contract during the final commutator. By a similar argument, the energy of $[[[[F, A_2], A_2], A_2], A_2]$ is incorrect in LCTSD but correct in QCTSD. Thus through a term by term analysis, QCTSD is shown to produce the correct energy for all contributions of order W^4 or lower. QCTSD does make errors of order W^5 , however, an example of which occurs in the term $[[[[W, A_2], A_2]_{1,2}, A_2], A_2]_{1,2}$. Here the three- and four-body operators neglected after the second commutator could have fully contracted during the outer two commutators. In conclusion, QCTSD is accurate to the same order in perturbation theory as CCSD, and thus we expect it to be more accurate than LCTSD when a single-determinant reference is employed.

G. Numerical stability

In general, the set of functions formed by applying excitation operators to a multireference wave function may be linearly degenerate. While CT theory must account for this, a more severe numerical problem arises from the decomposition of operators and density matrices. Examining the Newton–Raphson method used to solve for the CT amplitudes illuminates this problem.

At each step in the iterative CT algorithm, new amplitudes are produced by solving Eq. (19). As in other multireference theories, excitation degeneracies may cause the Jacobian matrix J to be singular. To repair J and orthonormalize the excitation basis, the Newton–Raphson equation is modified by the projected overlap matrix S , as shown in Eq. (33).

$$(S^{-1/2} J S^{-1/2}) S^{1/2} (\vec{x}_{i+1} - \vec{x}_i) = -S^{-1/2} \vec{r}_i. \quad (33)$$

S is computed by removing eigenvalues smaller than some threshold from the full overlap matrix. As the linear degeneracies correspond to these eigenvalues, Eq. (33) should be invertible. However, in CT theory there are additional difficulties.

If no approximations were made, the largest and smallest eigenvalues of the orthonormalized Jacobian $\tilde{J} = S^{-1/2} J S^{-1/2}$ would be roughly bound by the energies of excitations involving one or two external orbitals. Examined independently, S and J have many small eigenvalues. In the product $S^{-1/2} J S^{-1/2}$, a delicate cancellation of these eigenvalues produces a spectrum obeying the aforementioned boundaries. As a result, Eq. (33) should have a modest condition number. However, the error introduced by operator decomposition in the calculation of J disrupts this cancellation, leading to unphysically small eigenvalues in \tilde{J} and an insoluble linear equation. Even without decomposition, the applications of J given by Eqs. (18) and (27) are approximations. We have verified, however, that even when these equations are replaced by the true expression for the Jacobian, operator decomposition still produces unphysically small eigenvalues. We therefore continue to use Eqs. (18) and (27) for their efficiency.

Our current solution to this numerical issue is based on the method used to remove linear degeneracies from the excitation basis. By raising the threshold below which overlap eigenvalues are discarded, we may circumvent the problem

of small-eigenvalue cancellation. In practice we choose two parameters, τ_1 and τ_2 , as thresholds for the singly and doubly external excitation spaces. Compared to the typical thresholds used to remove linear degeneracies ($\sim 10^{-6}$), the thresholds necessary to repair the CT Jacobian are quite large ($\sim 10^{-2}$).

While the introduction of large thresholds makes CT theory tractable, they represent free parameters that have no physical justification. In Sec. IV E we present a practical approach for choosing the thresholds that helps remove their ambiguity. This method has proven successful in N_2 and H_2O , but a more robust approach is clearly desirable. Future research will investigate alternative methods for dealing with CT's numerical instabilities.

III. METHODS: AUTOMATIC ALGEBRA

The most difficult part of implementing a CT algorithm is deriving and encoding the tensor contractions necessary to compute the commutator approximations. Rather than deriving all the terms for the new methods by hand, we instead wrote a program to automate the process. This program, which may be downloaded via the link available in the supplemental information, performs the following tasks.

- (1) Expand all commutators;
- (2) normal order all operators;
- (3) apply operator/RDM decompositions; and
- (4) combine like terms.

While the first three operations are relatively straightforward, the fourth is difficult due to the high symmetry of the tensors involved and the freedom to rename dummy indices. As an example, consider the term shown in Eq. (34), which occurs when evaluating $[[H,A],A]_{1,2}$.

$$\sum_{\substack{a_1 a_2 a_3 \\ i_1 i_2 i_3 i_4 i_5}} \gamma_3^{a_3} \gamma_{i_3}^{j_4 a_1} v_{i_3 i_5}^{i_2 i_4} A_{a_2}^{a_1} A_{i_2 i_1}^{a_2 a_3}. \quad (34)$$

The tensors in this term have two-, eight-, eight-, one-, and fourfold symmetries for a total of 512 possible index arrangements. Further, because of the summation, all the indices are dummy indices.

In order to combine like terms, the program first transforms each term into a unique canonical form (here the word canonical has no relation to CT theory). The rules for writing a term in canonical form are based on a lexicographic ordering of the tensors and their indices, with some special conditions in the case of a repeated tensor name. This choice of canonical form is arbitrary and certainly not unique. What is important is that for each term encountered in CT theory, there is only one way to write it in canonical form. The canonical form for our example term is shown in Eq. (35)

$$\sum_{\substack{abcd \\ efgh}} A_b^a A_{de}^{bc} \gamma_f^c \gamma_{dh}^{ag} v_{fh}^{eg}. \quad (35)$$

To demonstrate why automatic derivations are necessary, Table II shows the number of unique terms required to evaluate the various commutators, assuming no factorization has

TABLE II. Evaluating commutators in CT theory requires many tensor contractions, the number of which are shown here for each type of commutator. See Sec. III for details.

Commutator	No. of unique terms
$[H,A]_{1,2}$	298
$[H,A]_{1,2,(3)}$	314
$[[H,A],A]_{1,2}$	16 935
$[[H,A],A]_{1,2,(3)}$	23 245
$\langle [H,\delta] \rangle_{1,2}$	110
$\langle [H,\delta] \rangle$	42
$\langle [[H,A],\delta] \rangle_{1,2}$	6552
$\langle [[H,A],\delta] \rangle_{1,2,(3)}$	10 504

been applied. The terms themselves can be found via the link in the supplemental information, along with the input files used to derive them. Once the terms have been derived, we use a separate program to generate the corresponding FORTRAN code.

IV. RESULTS

All results for methods other than CT were computed using the MOLPRO program package,^{13,19,20,57-62} with the exception of full configuration interaction (FCI) in N_2 , for which we use the results of Larsen *et al.*⁶³ All calculations are performed on singlet ground states. In BH and HF we compare methods based on a single-determinant reference function, while in H_2O and N_2 we compare multireference methods.

A. Boron hydride

The first molecule we study is BH, which is treated in the Dunning double zeta with polarization (DZP) basis⁶⁴ using Cartesian d orbitals, with the boron d orbital exponent changed to 0.5 as in Ref. 26. We have carried out two types of CT calculations, one using the Hartree-Fock determinant as the reference function and the other using a four-electron three-orbital ($4e, 3o$) CASSCF reference. In both cases, all electrons were correlated. Notice that when a single determinant is used as the CT reference function, the large truncation thresholds discussed in Sec. II G are unnecessary as the overlap matrices' eigenvalues are either 0 or ≥ 1 . Also recall that the cumulant approximation is exact for a single determinant, so the L3CTSD and Q3CTSD methods become redundant.

One reason for developing the QCTSD method was to improve accuracy when the reference function is a single electronic determinant. Figure 1 and Table III show that QCTSD is indeed an improvement over LCTSD when the Hartree-Fock reference is used. QCTSD is also an improvement when starting from the CASSCF solution, although this behavior appears to be unique to the BH molecule. In our other systems, QCTSD appears to be less accurate than LCTSD when a CASSCF solution is used as the reference function. We also note that QCTSD behaves similarly to CCSD when the Hartree-Fock reference is employed, as may be expected from the fact that their energies are formally accurate to the same order in the fluctuation potential. This similarity is most pronounced near the equilibrium ge-

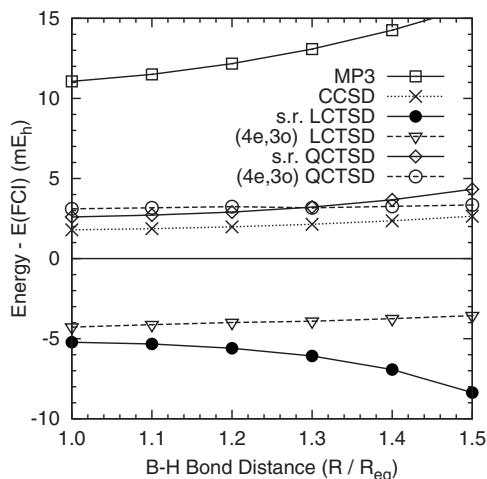


FIG. 1. Energy errors for BH in a modified DZP basis set. $R_{\text{eq}} = 2.329$ Bohr. $\tau_1 = \tau_2 = 0.05$. s.r. = single reference.

ometry. As the bond is stretched, QCTSD shows a larger nonparallelity error (NPE). Overall, the BH molecule supports the analysis that QCTSD should be more accurate than LCTSD when a single-determinant reference is used.

B. Hydrogen fluoride

HF is treated in the Dunning DZP basis⁶⁴ using spherical d orbitals, with the hydrogen p and fluorine d orbital exponents changed to 0.75 and 1.6, respectively, as in Ref. 26. We carried out CT calculations using both Hartree–Fock and $(2e, 2o)$ CASSCF solutions as reference functions. All orbitals were correlated.

QCTSD again makes an improvement on LCTSD when using the Hartree–Fock reference, as shown in Fig. 2 and Table IV. Its energy is also again very similar to CCSD, although it fails to converge for bond lengths greater than 150% of the equilibrium distance (both CT methods converge across the entire dissociation curve when using the CASSCF reference).

The main difference from BH can be seen when using a CASSCF reference function where, unlike in the Hartree–Fock case, QCTSD is less accurate than LCTSD. This unexpected behavior is also displayed in the H_2O and N_2 molecules. While LCTSD and QCTSD both enjoy improvements in absolute error when moving from a Hartree–Fock to

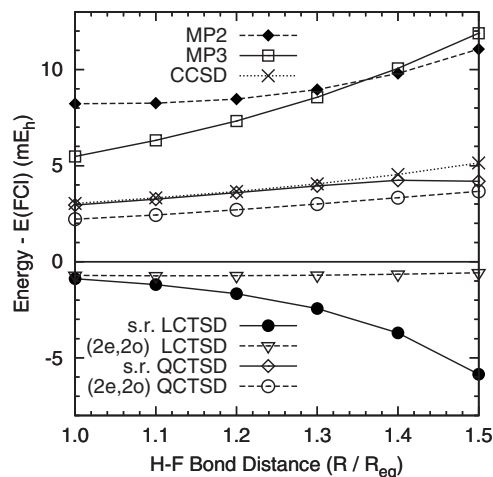


FIG. 2. Energy errors for HF in a modified DZP basis set. $R_{\text{eq}} = 1.733$ Bohr. $\tau_1 = \tau_2 = 0.001$. s.r. = single reference.

CASSCF reference, the improvements in LCTSD produce better parallelity with the FCI bonding curve.

C. Water

The H_2O molecule is treated in the Dunning cc-pVDZ basis set⁶⁵ using spherical d orbitals. The oxygen $1s$ orbital is frozen after the $(6e, 5o)$ CASSCF calculation. In this section we consider the symmetric stretching of the two O–H bonds. All dynamic correlation calculations employ the CASSCF reference function.

The most notable result in the water molecule is that QCTSD and Q3CTSD, which use the quadratic commutator approximation, are less accurate than LCTSD and L3CTSD, which use the linear commutator approximation. This can be seen in the nonparallelity errors shown in Table V and Fig. 3. The error in QCTSD, and to a lesser extent Q3CTSD, increases as the bonds are stretched up to 150% of their equilibrium distances, beyond which the error diminishes. This behavior is similar to that of CASPT3. In contrast, the errors for LCTSD and L3CTSD are less sensitive to the O–H bond distance, producing curves more parallel to FCI. A less surprising result is that the L3CTSD and Q3CTSD methods show superior parallelity as compared to LCTSD and QCTSD, respectively.

TABLE III. Results for BH in a modified DZP basis. FCI is reported in E_h , with other methods reported as the difference from FCI in mE_h . The Hartree–Fock solution is used as a reference except in the second set of CT calculations, which use a $(4e, 3o)$ CASSCF solution.

R/R_{eq}^a	FCI	HF	MP2	MP3	CCSD	LCTSD H-F	QCTSD H-F	LCTSD ^b (4e,3o)	QCTSD ^b (4e,3o)
1.0	-25.227 627	102.366	28.639	11.060	1.792	-5.225	2.595	-4.274	3.105
1.1	-25.223 980	103.563	29.430	11.502	1.868	-5.333	2.712	-4.124	3.170
1.2	-25.214 410	105.299	30.553	12.166	1.980	-5.595	2.906	-3.987	3.239
1.3	-25.202 124	107.575	32.029	13.077	2.140	-6.084	3.213	-3.912	3.173
1.4	-25.188 960	110.393	33.875	14.258	2.360	-6.930	3.672	-3.752	3.258
1.5	-25.175 976	113.763	36.107	15.727	2.644	-8.366	4.331	-3.562	3.352
NPE ^c	N/A	11.397	7.468	4.667	0.852	3.141	1.736	0.712	0.247

^a $R_{\text{eq}} = 2.329$ bohrs.

^b $\tau_1 = \tau_2 = 0.05$.

^cNonparallelity error.

TABLE IV. Results for HF in a modified DZP basis. FCI is reported in E_h , with other methods reported as the difference from FCI in mE_h . The Hartree–Fock solution is used as a reference except in the second set of CT calculations, which use a $(2e, 2o)$ CASSCF solution.

R/R_{eq}^a	FCI	HF	MP2	MP3	CCSD	LCTSD H–F	QCTSD H–F	LCTSD ^b ($2e, 2o$)	QCTSD ^b ($2e, 2o$)
1.0	−100.264 981	217.894	8.226	5.477	3.036	−0.881	2.951	−0.712	2.214
1.1	−100.257,467	221.981	8.249	6.314	3.322	−1.187	3.255	−0.729	2.436
1.2	−100.240,154	226.213	8.465	7.326	3.656	−1.666	3.596	−0.727	2.701
1.3	−100.218,661	230.720	8.956	8.558	4.056	−2.434	3.950	−0.701	3.005
1.4	−100.196,105	235.613	9.800	10.062	4.542	−3.700	4.238	−0.648	3.335
1.5	−100.174,219	240.989	11.062	11.889	5.137	−5.857	4.185	−0.575	3.663
NPE ^c	N/A	23.095	2.836	6.412	2.101	4.976	1.287	0.154	1.449

^a $R_{eq}=1.733$ bohrs.^b $\tau_1=\tau_2=0.001$.^cNonparallelity error.

Compared to CASPT2, the CT methods all show superior accuracy. This comparison is especially significant for LCTSD, as it has a lower cost scaling than multireference perturbation theory. Furthermore, LCTSD and L3CTSD are comparable in accuracy to the corrected MRCI methods (in fact, both LCTSD and L3CTSD are superior in accuracy to AQCC), while QCTSD and Q3CTSD are slightly lower in accuracy.

D. Nitrogen

The N_2 molecule is treated in the Dunning cc-pVDZ basis set⁶⁵ using spherical d orbitals. The $1s$ orbitals are frozen after the $(6e, 6o)$ CASSCF calculation, which is used as the reference for all dynamic correlation methods. Results for nitrogen are displayed in Table VI and Fig. 4.

As in the water molecule, the QCTSD method proves to be less accurate than LCTSD, displaying a larger nonparallelity error. It again shows an increase in energy relative to FCI during initial bond stretching, followed by a decrease as the bond is stretched further. The LCTSD method also displays this behavior, but to a lesser extent.

Unlike for water, the Q3CTSD method is more accurate than LCTSD and L3CTSD, showing the best parallelity of all methods tested. This is significant because even though Q3CTSD is more expensive than the other CT methods, it has a lower cost scaling than MRCI.

Including the exact three-body RDM improves CT's parallelity in N_2 , just as it did for H_2O . The improvement is

most notable in Q3CTSD, where the inclusion of the three-body RDM removes the energy error bump seen in QCTSD.

All CT methods were significantly more accurate than CASPT2, and all but QCTSD were competitive with the MRCI based methods. LCTSD, L3CTSD, and Q3CTSD showed NPEs of 1.9, 1.2, and 0.6 mE_h , respectively, compared to 1.0–1.3 mE_h for the corrected MRCI methods and 8.3 mE_h for CASPT2.

E. Truncation thresholds

This section investigates the effect of the thresholds τ_1 and τ_2 in the H_2O and N_2 molecules. The basis sets and frozen cores are the same as above.

Before discussing our results, we should point out how the overlap matrix is computed. In the spirit of CT theory, it is tempting to approximate the three-body RDMs needed to calculate the overlap matrix using the cumulant decomposition of Eq. (7). In practice this leads to less accurate energies, and so all calculations reported in this paper compute the overlap matrix using the true three-body RDM. This procedure eliminates what should be one of CT theory's advantages: requiring only the one- and two-body RDMs. Future research will attempt to remove the need for overlap thresholds entirely in order to recover this advantage.

Our current strategy is to use the smallest thresholds for which the CT equations are solvable and to use the same thresholds for all geometries. The reason for this choice is that the orthonormalized Jacobian's condition number should be physically bound (see Sec. II G). If the CT equations do

TABLE V. Results for the simultaneous bond breaking of H_2O using the cc-pVDZ basis set. FCI is reported in E_h , with other methods reported as the difference from FCI in mE_h . All dynamic correlation methods use the $(6e, 5o)$ CASSCF solution as a reference.

R/R_{eq}^a	FCI	CASSCF	CASPT2	CASPT3	MRCI	MRCI+Q	ACPF	AQCC	LCTSD ^b	L3CTSD ^b	QCTSD ^b	Q3CTSD ^b
1.0	−76.238 851	162.986	13.302	3.767	5.557	−0.561	0.933	2.313	−0.768	−1.232	2.680	2.387
1.5	−76.061 811	149.701	11.282	4.783	5.081	−0.572	0.876	2.133	−0.907	−1.783	3.509	2.795
2.0	−75.945 588	131.954	8.431	3.835	3.781	−0.525	0.542	1.504	−1.279	−1.510	1.933	1.712
2.5	−75.915 266	124.574	8.301	2.233	3.105	−0.639	0.257	1.100	−1.829	−1.865	0.733	0.700
3.0	−75.910 028	123.011	8.464	1.721	2.946	−0.673	0.184	1.001	−1.919	−1.923	0.371	0.368
NPE ^c	N/A	39.975	5.091	3.061	2.661	0.169	0.757	1.335	1.152	0.691	3.138	2.427

^a $R_{eq}=1.876$ bohrs, $\angle HOH=109.57^\circ$.^b $\tau_1=\tau_2=0.01$.^cNonparallelity error.

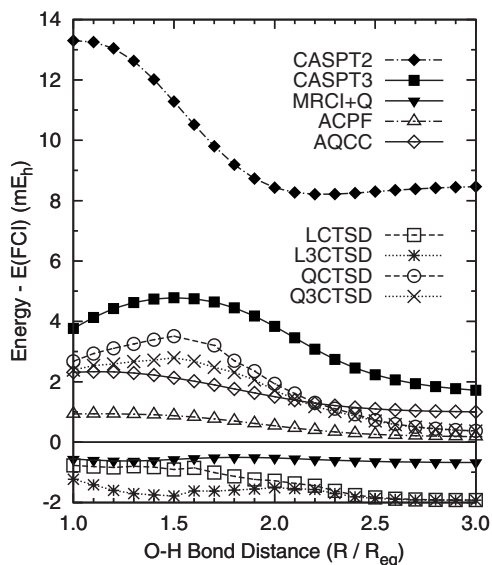


FIG. 3. Energy errors for the simultaneous bond breaking of H_2O in the cc-pVDZ basis set. $R_{\text{eq}}=1.876$ Bohr. Bond angle= 109.57° . $\tau_1=\tau_2=0.01$.

not converge, we interpret it as an indication that CT's approximations are preventing the necessary small-eigenvalue cancellation between the Jacobian and overlap matrix, and thus raise the truncation threshold to remove the small overlap eigenvalues. This approach should not be viewed as a rigorous justification for our choice of thresholds, but rather as a pragmatic method for setting threshold values.

In H_2O , for example, the LCTSD equations did not converge at all points for thresholds below $\tau_1=\tau_2=0.01$. While the CT equations can be solved for some geometries with smaller thresholds, we use 0.01 in an effort to maintain a balanced description. For N_2 , the minimum convergable LCTSD thresholds were $\tau_1=0.02$ and $\tau_2=0.01$.

Figure 5 shows the effects of choosing different thresholds close to the minimum convergable threshold on the LCTSD and QCTSD energies for H_2O . For O–H bond distances greater than 150% of equilibrium, changing the thresholds has only minor (<1 mE_h) effects on the energy. For distances between 100% and 150%, the thresholds' ef-

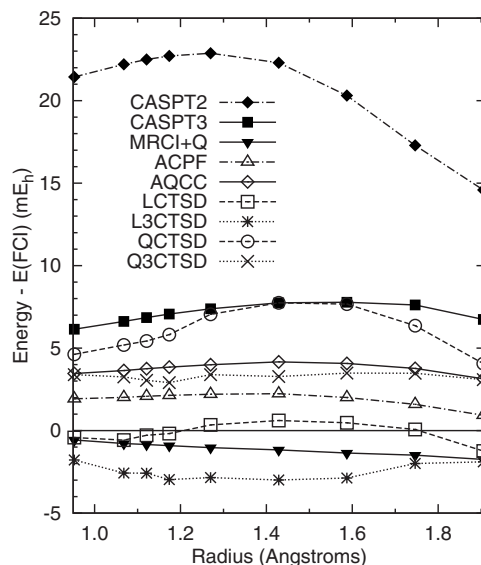


FIG. 4. Energy errors for the bond breaking of N_2 in the cc-pVDZ basis set. $\tau_1=0.02$ and $\tau_2=0.01$.

fects are as large as $2mE_h$. It is encouraging to observe that the smallest convergable threshold gives the smoothest curves for both LCTSD and QCTSD.

Figure 6 shows threshold dependence for N_2 . For LCTSD, the change in energy with thresholds was <1 mE_h at all geometries. The QCTSD energy was more sensitive to the choice of threshold, showing energy changes of up to 2.5 mE_h . We note that again, the lowest convergable thresholds yield the smoothest energy curve.

F. Summary

As expected in the single-reference tests (BH and HF), QCTSD improved on the accuracy of LCTSD, giving results comparable to CCSD. In the multireference tests (H_2O and N_2), QCTSD was less accurate than LCTSD but L3CTSD was more accurate. All CT methods were significantly more accurate than CASPT2 in the multireference tests, while LCTSD and especially L3CTSD had accuracies competitive with ACPF, AQCC, and MRCI+Q.

TABLE VI. Results for the bond breaking of N_2 using the cc-pVDZ basis set. FCI is reported in E_h , with other methods reported as the difference from FCI in mE_h . All dynamic correlation methods use the $(6e,6o)$ CASSCF solution as a reference.

R^a	FCI ^b	CASSCF	CASPT2	CASPT3	MRCI	MRCI+Q	ACPF	AQCC	LCTSD ^c	L3CTSD ^c	QCTSD ^c	Q3CTSD ^c
0.9525	-109.167 573	182.072	21.437	6.146	8.391	-0.564	1.932	3.458	-0.421	-1.781	4.620	3.387
1.0679	-109.270 384	186.030	22.202	6.618	8.883	-0.782	2.016	3.642	-0.576	-2.575	5.191	3.257
1.1208	-109.278 339	187.644	22.497	6.852	9.123	-0.845	2.083	3.752	-0.281	-2.582	5.426	3.043
1.1737	-109.271 915	189.155	22.713	7.062	9.348	-0.812	2.136	3.847	-0.178	-2.696	5.818	2.913
1.2700	-109.238 397	191.715	22.873	7.387	9.734	-1.029	2.207	3.996	0.342	-2.852	7.044	3.387
1.4288	-109.160 305	195.376	22.300	7.743	10.313	-1.174	2.240	4.165	0.613	-2.993	7.745	3.280
1.5875	-109.086 211	197.685	20.309	7.782	10.634	-1.363	2.004	4.069	0.474	-2.873	7.672	3.485
1.7463	-109.030 31	197.660	17.287	7.616	10.664	-1.491	1.591	3.768	0.070	-1.995	6.359	3.473
1.9050	-108.994 81	194.696	14.587	6.740	10.140	-1.750	0.928	3.142	-1.241	-1.891	4.066	3.086
NPE ^d	N/A	15.612	8.286	1.635	2.272	1.186	1.312	1.023	1.854	1.213	3.679	0.571

^aRadii in angstroms.

^bFCI results of Larsen *et al.* (Ref. 63).

^c $\tau_1=0.02$ and $\tau_2=0.01$.

^dNonparallelity error.

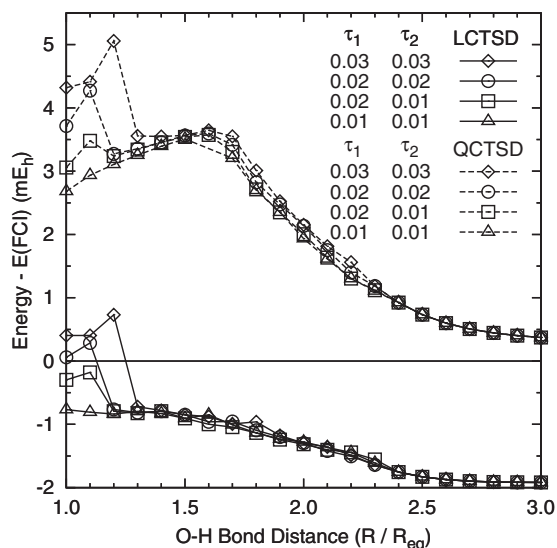


FIG. 5. Effect of the overlap truncation thresholds τ_1 and τ_2 on the simultaneous bond breaking of H_2O in the cc-pVDZ basis set. $R_{\text{eq}}=1.876$ Bohr. Bond angle= 109.57° .

V. CONCLUSIONS

CT theory uses a unitary exponential ansatz, a Hermitian effective Hamiltonian, and commutator approximations to efficiently model dynamic correlation in multireference systems. It is rigorously size extensive and demonstrates an accuracy superior to CASPT2 and competitive with the corrected MRCI methods ACPF, AQCC, and MRCI+Q. Here we developed and tested several extensions to the original linear CT with singles and doubles (LCTSD) method, namely, quadratic CT (QCTSD), and linear and quadratic CT with the three-body reduced density matrix (L3CTSD, Q3CTSD). Our results show that while LCTSD provides a good balance between cost and accuracy, there are two cases where our newer methods are preferable. First, for systems where it is practical to compute the three-body reduced density matrix, the L3CTSD method provides a further increase

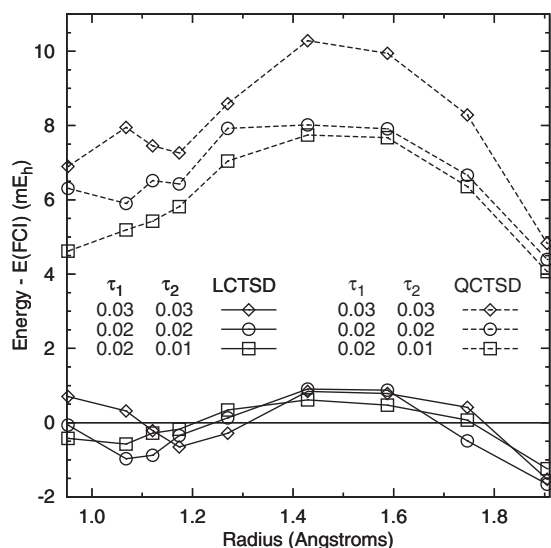


FIG. 6. Effect of the overlap truncation thresholds τ_1 and τ_2 on the bond breaking of N_2 in the cc-pVDZ basis set.

in accuracy over the LCTSD method. While L3CTSD has a cost scaling higher than LCTSD (n^7 versus n^6), this is still lower than CASPT2 or MRCI. Second, when the reference function is a single Slater determinant, QCTSD has an accuracy that is superior to LCTSD both formally and in practice.

While the accuracy and performance characteristics of the CT methods are quite favorable, the numerical difficulties associated with solving the CT amplitude equations remain unresolved. Although we have shown that these can be dealt with in a practical manner, a more robust solution would greatly improve reliability. Current research is therefore focused on addressing these numerical issues.

ACKNOWLEDGMENTS

This work was supported by Cornell University, the National Science Foundation under CAREER Program No. CHE-0645380, and the Department of Energy Office of Science under Award No. DE-FG02-07ER46432. E.N. would like to acknowledge the support of the National Science Foundation Graduate Research Fellowship Program.

- K. Ruedenberg, M. W. Schmidt, M. M. Gilbert, and S. T. Elbert, *Chem. Phys.* **71**, 41 (1982).
- B. O. Roos, *Adv. Chem. Phys.* **69**, 399 (1987).
- S. R. White and R. L. Martin, *J. Chem. Phys.* **110**, 4127 (1999).
- G. K.-L. Chan and M. Head-Gordon, *J. Chem. Phys.* **116**, 4462 (2002).
- J. Hachmann, W. Cardoen, and G. K.-L. Chan, *J. Chem. Phys.* **125**, 144101 (2006).
- D. Ghosh, J. Hachmann, T. Yanai, and G. K.-L. Chan, *J. Chem. Phys.* **128**, 144117 (2008).
- K. H. Marti, I. M. Ondík, G. Moritz, and M. Reiher, *J. Chem. Phys.* **128**, 014104 (2008).
- R. J. Bartlett and J. F. Stanton, *Rev. Comput. Chem.* **5**, 65 (1994).
- T. J. Lee and G. E. Scuseria, in *Quantum Mechanical Electronic Structure Calculations with Chemical Accuracy*, edited by S. R. Langhoff (Kluwer Academic, Dordrecht, 1995), Vol. 2, pp. 47–108.
- T. Helgaker, T. A. Ruden, P. Jørgensen, J. Olsen, and W. Klopper, *J. Phys. Org. Chem.* **17**, 913 (2004).
- K. Andersson, P.-Å. Malmqvist, B. O. Roos, A. J. Sadlej, and K. Wolinski, *J. Phys. Chem.* **94**, 5483 (1990).
- K. Andersson, P.-Å. Malmqvist, and B. O. Roos, *J. Chem. Phys.* **96**, 1218 (1992).
- P. Celani and H.-J. Werner, *J. Chem. Phys.* **112**, 5546 (2000).
- K. Hirao, *Chem. Phys. Lett.* **190**, 374 (1992).
- C. Angeli, R. Cimraglia, S. Evangelisti, T. Leininger, and J.-P. Malrieu, *J. Chem. Phys.* **114**, 10252 (2001).
- C. Angeli, R. Cimraglia, and J.-P. Malrieu, *J. Chem. Phys.* **117**, 9138 (2002).
- N. Forsberg and P.-Å. Malmqvist, *Chem. Phys. Lett.* **274**, 196 (1997).
- H.-J. Werner and E. A. Reinsch, *J. Chem. Phys.* **76**, 3144 (1982).
- H.-J. Werner and P. J. Knowles, *J. Chem. Phys.* **89**, 5803 (1988).
- P. J. Knowles and H.-J. Werner, *Chem. Phys. Lett.* **145**, 514 (1988).
- S. R. Langhoff and E. R. Davidson, *Int. J. Quantum Chem.* **8**, 61 (1974).
- E. R. Davidson and D. W. Silver, *Chem. Phys. Lett.* **52**, 403 (1977).
- R. J. Gdanitz and R. Ahlrichs, *Chem. Phys. Lett.* **143**, 413 (1988).
- H.-J. Werner and P. J. Knowles, *Theor. Chim. Acta* **78**, 175 (1990).
- P. G. Szalay and R. J. Bartlett, *Chem. Phys. Lett.* **214**, 481 (1993).
- T. Yanai and G. K.-L. Chan, *J. Chem. Phys.* **124**, 194106 (2006).
- T. Yanai and G. K.-L. Chan, *J. Chem. Phys.* **127**, 104107 (2007).
- G. Kin-Lic Chan and T. Yanai, *Adv. Chem. Phys.* **134**, 343 (2007).
- W. Kutzelnigg, *J. Chem. Phys.* **77**, 3081 (1982).
- W. Kutzelnigg, *J. Chem. Phys.* **80**, 822 (1984).
- J. D. Watts, G. W. Trucks, and R. J. Bartlett, *Chem. Phys. Lett.* **157**, 359 (1989).
- R. J. Bartlett, S. A. Kucharski, and J. Noga, *Chem. Phys. Lett.* **155**, 133 (1989).
- A. G. Taube and R. J. Bartlett, *Int. J. Quantum Chem.* **106**, 3393 (2006).
- S. Pal, M. D. Prasad, and D. Mukherjee, *Theor. Chim. Acta* **62**, 523

- (1983).
- ³⁵ S. Pal, *Theor. Chim. Acta* **66**, 207 (1984).
- ³⁶ J. Paldus and X. Li, *Adv. Chem. Phys.* **110**, 1 (1999).
- ³⁷ M. R. Hoffmann and J. Simons, *J. Chem. Phys.* **88**, 993 (1988).
- ³⁸ K. F. Freed, in *Many-Body Methods in Quantum Chemistry*, edited by U. Kaldor (Springer, Berlin, 1989), p. 1.
- ³⁹ B. Kirtman, *J. Chem. Phys.* **75**, 798 (1981).
- ⁴⁰ S. R. White, *J. Chem. Phys.* **117**, 7472 (2002).
- ⁴¹ W. Kutzelnigg and D. Mukherjee, *J. Chem. Phys.* **107**, 432 (1997).
- ⁴² D. Mukherjee, *Chem. Phys. Lett.* **274**, 561 (1997).
- ⁴³ D. Mukherjee, in *Recent Progress in Many-Body Theories*, edited by E. Schachinger (Plenum, New York, 1995), Vol. 4, p. 127.
- ⁴⁴ F. Colmenero and C. Valdemoro, *Phys. Rev. A* **47**, 979 (1993).
- ⁴⁵ W. Kutzelnigg and D. Mukherjee, *J. Chem. Phys.* **110**, 2800 (1999).
- ⁴⁶ H. Nakatsuji and K. Yasuda, *Phys. Rev. Lett.* **76**, 1039 (1996).
- ⁴⁷ D. A. Mazziotti, *Phys. Rev. A* **57**, 4219 (1998).
- ⁴⁸ L. Cohen and C. Frishberg, *Phys. Rev. A* **13**, 927 (1976).
- ⁴⁹ H. Nakatsuji, *Phys. Rev. A* **14**, 41 (1976).
- ⁵⁰ F. E. Harris, *Int. J. Quantum Chem.* **90**, 105 (2002).
- ⁵¹ J. M. Herbert, *Int. J. Quantum Chem.* **107**, 703 (2007).
- ⁵² D. A. Mazziotti, *Phys. Rev. Lett.* **97**, 143002 (2006).
- ⁵³ D. A. Mazziotti, *Phys. Rev. A* **75**, 022505 (2007).
- ⁵⁴ A. E. DePrince III and D. A. Mazziotti, *J. Chem. Phys.* **127**, 104104 (2007).
- ⁵⁵ W. Kutzelnigg, *Chem. Phys. Lett.* **64**, 383 (1979).
- ⁵⁶ R. J. Bartlett, S. A. Kucharski, J. Noga, J. D. Watts, and G. W. Trucks, in *Many-Body Methods in Quantum Chemistry*, edited by U. Kaldor (Springer, Berlin, 1989), p. 125.
- ⁵⁷ H.-J. Werner, *Mol. Phys.* **89**, 645 (1996).
- ⁵⁸ C. Hampel, K. A. Peterson, and H.-J. Werner, *Chem. Phys. Lett.* **190**, 1 (1992).
- ⁵⁹ P. J. Knowles and N. C. Handy, *Chem. Phys. Lett.* **111**, 315 (1984).
- ⁶⁰ P. J. Knowles and N. C. Handy, *Comput. Phys. Commun.* **54**, 75 (1989).
- ⁶¹ H.-J. Werner and P. J. Knowles, *J. Chem. Phys.* **82**, 5053 (1985).
- ⁶² P. J. Knowles and H.-J. Werner, *Chem. Phys. Lett.* **115**, 259 (1985).
- ⁶³ H. Larsen, J. Olsen, P. Jørgensen, and O. Christiansen, *J. Chem. Phys.* **113**, 6677 (2000).
- ⁶⁴ T. H. Dunning, *J. Chem. Phys.* **53**, 2823 (1970).
- ⁶⁵ T. H. Dunning, *J. Chem. Phys.* **90**, 1007 (1989).